HHS Public Access

Author manuscript

J Control Release. Author manuscript; available in PMC 2020 October 01.

Published in final edited form as:

J Control Release. 2019 October ; 311-312: 273–287. doi:10.1016/j.jconrel.2019.09.006.

Bioengineered Adipose-Derived Stem Cells for Targeted Enzyme-Prodrug Therapy of Ovarian Cancer Intraperitoneal Metastasis

Obeid M. Malekshah[1], **Siddik Sarkar**[1], **Alireza Nomani**[1], **Niket Patel**[1], **Parisa Javidian**[2], **Michael Goedken**[3], **Marianne Polunas**[3], **Pedro Louro**[3], **Arash Hatefi**[*,1,4]

[1]Department of Pharmaceutics, Rutgers University, Piscataway, New Jersey 08854, USA

[2]Department of Pathology and Laboratory Medicine, Rutgers-Robert Wood Johnson Medical School, New Brunswick, New Jersey 08903, USA

[3]Rutgers Research Pathology Services, Rutgers University, Piscataway, 08854, New Jersey, USA

[4]Cancer Pharmacology Program, Rutgers-Cancer Institute of New Jersey, New Brunswick, New Jersey 08903, USA

Abstract

The objective of this study was to develop a stem cell-based system for targeted suicide gene therapy of recurrent, metastatic, and unresectable ovarian cancer. Malignant cells were obtained from the ascites of a patient with advanced recurrent epithelial ovarian cancer (named OVASC-1). Cancer cells were characterized to determine the percentages of drug-resistant ALDH+ cells, MDR-1/ABCG2 overexpressing cells, and cancer stem-like cells. The sensitivity and resistance of the OVASC-1 cells and spheroids to the metabolites of three different enzyme/prodrug systems were assessed, and the most effective one was selected. Adipose-derived stem cells (ASCs) were genetically engineered to express recombinant secretory human carboxylesterase-2 and nanoluciferase genes for simultaneous disease therapy and quantitative imaging. Bioluminescent imaging, magnetic resonance imaging and immuno/histochemistry results show that the engineered ASCs actively targeted and localized at both tumor stroma and necrotic regions. This created the unique opportunity to deliver drugs to not only tumor supporting cells in the stroma, but also to cancer stem-like cells in necrotic/hypoxic regions. The statistical analysis of intraperitoneal OVASC-1 tumor burden and survival rates in mice shows that the administration of the bioengineered ASCs in combination with irinotecan prodrug in the designed sequence and timeline eradicated all intraperitoneal tumors and provided survival benefits. In contrast, treatment of the drug-resistant OVASC-1 tumors with cisplatin/paclitaxel (standard-of-care) did not have any statistically significant benefit. The histopathology and hematology results do not show any

[*]Correspondence should be addressed to: Arash Hatefi (PharmD, PhD), Department of Pharmaceutics, Room 222, Rutgers University, 160 Frelinghuysen Road, Piscataway, NJ 08854-8020, Tel: 848-445-6366, Fax: 732-445-3134, ahatefi@pharmacy.rutgers.edu.

Declarations of Interests

None

toxicity to major peritoneal organs. Our toxicity data in combination with efficacy outcomes delineate a nonsurgical and targeted stem cell-based approach to overcoming drug resistance in recurrent metastatic ovarian cancer.

Keywords

Adipose Derived Mesenchymal Stem Cells; Suicide Gene Therapy; Ovarian Cancer; Targeted Therapy; Enzyme Prodrug Systems

Introduction

The majority of the ovarian cancer patients do not experience symptoms in early stages of the disease and are diagnosed in late stages once cancer cells have leaked into the peritoneum and metastasized into organs outside of the ovaries. The standard-of-care for such patients includes cytoreductive surgery followed by chemotherapy with platinum-based drugs (e.g., cisplatin or carboplatin) and paclitaxel (PTX) [1]. Unfortunately, approximately 90% of patients after suboptimal resection and 70% of patients after optimal cytoreduction go on to experience relapse within 18–24 months [2, 3]. While a standard therapeutic approach for these patients with drug-resistant recurrent disease has not been established, chemotherapy regimens using agents other than cisplatin/PTX such as topotecan [4, 5], irinotecan (CPT-11) [6, 7], liposomal doxorubicin [8, 9], etoposide [10, 11], gemcitabine [12], and ifosfamide [10] have been employed yielding response rates of between 10% and 30%; however, no survival benefit has been observed [13]. The prognosis is even poorer for patients with recurrent metastatic disease who have unresectable tumors and who are not candidates for surgery. Therefore, *the objective* of this study was to develop a nonsurgical targeted therapeutic approach that can be used for the treatment of patients with intraperitoneal metastasis of drug-resistant ovarian cancer.

In the past decades many studies have shown that drug-resistant ovarian cancer cells can be killed under in vitro conditions when exposed to high concentrations of anticancer drugs. Our group has shown that cisplatin given at 100 μM and SN-38 at 100 nM concentrations can completely eradicate drug-resistant ovarian tumorspheres in the cell culture [14], However, the main problem faced concerns the fact that such high effective drug doses cannot be easily delivered to tumors due to the resulting dose-limiting toxicity to healthy tissues. If we could devise a means to simulate in vitro conditions in vivo, it would then be possible to effectively kill drug-sensitive and -resistant cancer cells and cure the disease. To achieve this goal, we took advantage of the inherent tumor tropism of mesenchymal stem cells (MSCs), which is driven by tumor-secreted cytokines [15]. We *hypothesized* that suicide gene expressing MSCs can actively migrate toward ovarian intraperitoneal tumors and convert prodrugs into their potent metabolites close to the tumor cells, resulting in their complete eradication. In turn, this should prolong survival rate and reduce toxicity to normal tissues. To test the hypothesis, we obtained ascites-derived malignant cells from a patient with advanced drug-resistant epithelial ovarian cancer (OVASC-1). The cells were characterized to identify factors contributing to their drug resistance. To treat OVASC-1 intraperitoneal tumors, ASCs were first genetically modified ex-vivo to express secretory

human carboxylesterase-2 (shCE2) enzyme. They were then injected into mice peritoneum to migrate toward OVASC-1 intraperitoneal tumors. Subsequently, irinotecan (prodrug) was administered to be converted into its cytotoxic form (SN-38) by the secreted CE2 [16, 17]. We utilized ASCs as enzyme delivery vehicles because these cells exhibit a high degree of inherent tropism toward ovarian tumors, thus helping us better direct the treatment to the tumors [18, 19]. The ASCs were also engineered to express nanoluciferase for cell tracking and quantitative therapy response analysis. The fate of ASCs after injection into the mice peritoneum (distribution and localization) was studied by bioluminescent imaging (BLI), magnetic resonance imaging (MRI), and immuno/histochemistry. The responses of tumors to therapy were studied by quantitative BLI and the survival benefit was measured. The adverse effects of therapy were evaluated by measuring the observable toxicity as well as histopathology and hematology.

Materials and Methods

Cell culture

All cancer cell lines were authenticated by the University of Arizona Genetics Core Cell Authentication Services. Low-grade ovarian cancer cell lines A2780 (Sigma-Aldrich, MO, USA) and SKOV-3 (ATCC, VA, USA) as well as drug-resistant ovarian cancer models A2780-Cis (cisplatin resistant, Sigma-Aldrich) and OVCAR-3 (ATCC) were purchased and cultured as per vendor's protocol Ascites-derived epithelial ovarian cancer cells (de-identified) were obtained from the Biorepository Center of Rutgers-Cancer Institute of New Jersey (passage 7). For simplicity, we named them OVASC-1 since they were originated from ovarian ascites. OVASC-1 cells were maintained in RPMI-1640 supplemented with 15% FBS and 2.5 μg/mL insulin The media was changed every other day. ASC cell line (ASC52telo, hTERT immortalized adipose-derived mesenchymal stem cells) (ATCC) was cultured in ASC basal medium supplemented with Mesenchymal Stem Cell Growth Kit (ATCC) and 0.2 mg/mL G418 (Sigma-Aldrich). To inhibit bacterial growth, 1% Penicillin-streptomycin solution (Caisson Labs, UT, USA) was added to the culture media of all cell lines.

Measurement of the sensitivity of the ovarian cancer cells to anticancer drugs

To measure the sensitivity of the ovarian cancer cells to the anticancer drugs, they were seeded in 96-well plates at a density of 5×10^3 cells/well. After twenty-four hours, cells were treated with a range of drug concentrations and then incubated at 37°C for 72 hours. Next, WST-1 reagent (Sigma-Aldrich) was added to each well and incubated for 2 hours. The absorbance of each well was measured at 440 nm The viability of untreated cells was considered as 100% and from that, the viabilities of other samples were calculated. The data are presented as mean±SD (n=4).

Clonogenic assay

The long-term toxic effects of anticancer drugs were evaluated by clonogenic assay. Briefly, 5×10^2 cells were seeded in 12-well plates and allowed to grow for 3 days. Then, they were treated with anticancer drugs at different concentrations. After incubation for 14 days, cells were washed with PBS and stained with 0.1% crystal violet solution The number of colonies

containing ≥ 50 cells was counted with an inverted light microscope. The data are presented as mean±SD (n=3).

Limiting dilution assay

To determine the frequency of the colony forming cells in each cancer cell population an in vitro limiting dilution assay (LDA) was performed. Ovarian cancer cells were trypsinized, diluted serially and then seeded in 96-well plates at different cell densities ranging from 1 to 500 cells/well (n=8). After incubation at 37 °C for 21 days, cells were washed twice with PBS and stained with 0.1% crystal violet solution (Sigma-Aldrich). The number of colonies containing ≥ 50 cells was counted with an inverted light microscope. Using the data, the frequency of the cancer initiating cells (CICs) in each ovarian cancer cell population was estimated by ELDA online software (http://bioinf.wehi.edu.au/software/elda/index.html) as previously described [20].

ALDH activity assay

The activity of aldehyde dehydrogenase enzyme (ALDH) in ovarian cancer cells was evaluated by using ALDEFLUOR™ kit and protocol (Stem Cell Technologies, BC, Canada). Ovarian cancer cells were grown in T-75 flasks, trypsinized and one million cells were counted. Half million cells were transferred into a microfuge tube and treated with diethylaminobenzaldehyde (DEAB) and ALDEFLUOR substrate. The same number of cells was counted and treated with ALDEFLUOR substrate only. Cells were incubated for 45 min at 37°C in the dark and then analyzed by Gallios Beckman Coulter Cytometer (Beckman Coulter, Inc., CA, USA). Gating was established using propidium iodide (PI) to exclude non-viable cells. ALDEFLUOR plus DEAB was used to determine the negative gates. Data analysis was conducted by using Kaluza® Flow Analysis software (Beckman Coulter, Inc.). The data are reported as mean±SD (n=3).

To measure the activity of ALDH enzyme in OVASC-1 and OVACR-3 cells that were treated with SN-38 and cisplatin, 1×10^6 cells were seeded in 6-well plates. After twenty-four hours, cells were treated with 1–100 μM of cisplatin or 1–100 nM of SN-38. After 72 hours of treatment, the ALDH enzymatic activity in the abovementioned ovarian cancer cell lines was measured by ALDEFLUOR kit as explained.

Measurement of MDR1 and ABCG2 cell surface transporters

To determine the cell surface expression levels of MDR1 and ABCG2 transporters, cells were seeded in 6-well plates and then incubated either with anti-MDR-1 primary (abcam, Cambridge, MA) (ab10333) and corresponding secondary antibody (ab150117), or anti-ABCG2 primary (ab207732) and secondary antibodies (ab150077). Flow cytometry analyses were performed on cells by using the Beckman Coulter Gallios Flow Cytometer. As negative controls, the staining procedure was performed by using IgG isotype controls (ab18413) and (ab172730) for MDR1 and ABCG2, respectively. The duration of antibody treatment and concentration were based on the vendor's protocol. Data are reported as the percentage of cells expressing each protein X-mean denotes the fold change in the mean fluorescent intensity of the test group in comparison to the corresponding IgG isotype. Data analysis was performed using Kaluza® Flow analysis software (Beckman Coulter, Inc).

Ovarian tumorsphere formation and characterization

To generate OVASC-1 tumorspheres, cells were seeded in ultra-low attachment 6-well plates (Coming Inc., NY, USA) at the density of 2×10^3 cells/well in MEBM (Lonza) supplemented with 0.4% bovine serum albumin (BSA) (Sigma-Aldrich), 20 ng/mL epidermal growth factor (EGF) (Invitrogen, NY, USA), 10 ng/mL basic fibroblast growth factor (bFGF) (Sigma-Aldrich), 5 μg/mL insulin, and 1% Penicillin-streptomycin solution The cells were incubated under the said conditions for five days until tumorspheres were formed.

To determine the expression levels of stem cell biomarkers, the tumorspheres were dissociated by trypsin and the total RNA was extracted from cells using RNeasy mini-kit (Qiagen, Hilden, Germany) according to the manufacturer's protocol. cDNA was prepared from the extracted RNA by High Capacity cDNA Reverse Transcription kit (Applied biosystems, CA, USA). Real-time PCR was performed using TaqMan gene expression assay kit (Applied biosystems) for stem cell-related genes of interest NANOG, SOX-2 and OCT-4. Primer probe numbers were catalog number Hs02758991_gl for human GAPDH; catalog number Hs04399610_gl for NANOG; catalog number Hs04234836_sl for SOX2 and catalog number AIKAMMD PN4331348 for OCT-4 (TaqMan® Gene Expression, Thermofischer scientific, MA, USA). All quantitative real-time PCR reactions were performed and analyzed using the StepOne Plus Real-Time PCR System (Applied Biosystems) with the comparative ΔCt method. The relative expression of genes with respect to the housekeeping gene human GAPDH are presented as mean±SD (n=4).

Measurement of tumorsphere diameter and viability

To evaluate the effects of anticancer drug treatment on tumorspheres, OVASC-1 tumorspheres were generated, treated once either with 1–100 μM of cisplatin or 1–100 nM of SN-38, and then incubated for 14 days. The diameters of the tumorspheres were measured under an Olympus light microscope by using Infinity Analysis software. Data are presented as mean±s.d. (n=4). The viability of the cells in tumorspheres was determined by fluorescence microscopy after staining with 2.5 (μM of Calcein AM (live cells) and 30 μM propidium iodide (dead cells) (Sigma-Aldrich) for 2 hours at 4°C.

Genetic engineering of ASCs

The genes encoding human carboxylesterase-2 (hCE2) and nanoluciferase (NanoLuc®, Promega, Madison, WI) were designed and then synthesized by VectorBuilder Inc. (Santa Clara, CA USA) for mammalian cell expression using PiggyBac transposon system The secretory form of human carboxylesterase-2 (shCE2) was generated by removing the ER retention signal (HTEL) from the non-secretory form (hCE2). This signal is encoded as 12 nucleotides (4 amino acids) located at the peptide's C-terminal. The ASCs were seeded in 6-well plates at the density of 3×10^5 cells/well and then co-transfected with the constructed transposon plasmid vectors along with helper plasmid encoding hyperactive PiggyBac transposase system by using XFECT™ reagent (Takara Bio, Inc., CA, USA) following the manufacturer's protocol. Transfected ASCs were maintained in full media supplemented with 400 μg/ml Hygromycin B (Clontech, CA USA) for 3–4 weeks to obtain the stable clones expressing carboxylesterase and nanoluciferase. The stable clones ASC-shCE2:nLuc

(secretory) and ASC-hCE2:nLuc (non-secretory) were generated, expanded and stored under liquid nitrogen for further use.

Evaluation of the activity of the expressed human carboxylesterase-2

ASC-shCE2:nLuc cells were seeded in 24-well plates at the density of 2.5×10^4 cells/well in 500 μl of complete culture media. After 24 hours, 100 μL of the media was collected and incubated with 100 μl of fluorescein diacetate (FDA) (12 μM). The fluorescent signal of byproduct (fluorescein) was measured for 30 min at 5 min interval by using Tecan plate reader instrument (Tecan, Männedorf, Switzerland), excitation/emission set at 485/535. Culture media was taken from ASC-hCE2:nLuc cells (non-secretory), culture media alone and PBS were used as controls.

The ability of the secreted carboxylesterase from ASC-shCE2:nLuc cells to convert irinotecan to SN-38 was examined by Liquid Chromatography-Mass Spectroscopy (LC/MS) at Biological Mass spectrometry core facility of the Rutgers-Robert Wood Johnson Medical school. ASC-shCE2:nLuc cells were seeded at the density of 2.5×10^4 cells/well in a 24-well plate with 500 μl of complete media. The next day, the culture media was removed from each well and treated once with 7.5 μM of irinotecan and then incubated for 72 hours at 37°C. Next, 100 μl of the treated media was mixed with 200 μl acetonitrile (Sigma-Aldrich) and centrifuged at 12000g for 10 min The resulted supernatant was mixed with 200 μl 1% formic acid (Sigma-Aldrich). 5 μl of the sample was loaded for LC/MS using nano-LC-MS/MS with the Dionex RSLC system (ThermoFisher) interfaced with a LTQ Orbitrap Velos (ThermoFisher). The HPLC column C18 3.5 μm, 2.1 mm × 50 mm was used with the flow rate of 0.2 mL/min. The mass spectrometer was set to do MSMS on 587.3 in an ion trap with collision energy 35 and isolation width 1.5 amu for irinotecan, and on 393.2 in an ion trap with collision energy 30 and isolation width 1.0 amu for SN-38. The summed intensity of fragment ions 543.3 and 502.25 were used for plotting and quantitation of irinotecan and the intensity of fragment ion 349.2 was used for plotting and quantitation of SN-38.

In vitro evaluation of the cancer cell killing efficiency of suicide gene expressing ASCs

ASC-shCE2:nLuc cells were co-cultured with OVASC-1 cells at the density of 1000 and 2500 cells/well After 24 hours, irinotecan (1 μM) was added to the media and incubated for an additional 72 hours. A cell viability assay was performed by using WST-1 reagent as described above. OVASC-1 cells and ASC-shCE2:nLuc cells seeded separately were used as controls. The viability of ASC-shCE2:nLuc cells co-cultured with OVASC-1 cells but without any irinotecan treatment was considered as 100% viable. The data are presented as mean±SD (n=4).

Evaluation of the ASC tumor tropism by BLI, MRI, and immune/histochemistry

All animal studies were performed according to the guidelines of the Rutgers University Institutional Animal Care and Use Committee (IACUC) and all experiments conformed to all relevant regulatory standards. Outbred homozygous nude J:NU (Foxn1nu/Foxn1nu) female mice (5–6 weeks old) were purchased from the Jackson Laboratory (Bar Harbor, ME). OVASC-1 cells that stably expressed firefly luciferase gene (OVASC-1-fLuc) were

created as described previously [14]. Five million OVASC-1-fLuc cells were suspended in 500 μL of D-PBS and injected intraperitoneally (IP) into nude mice using a 25-gauge needle. The cancer cells were left to grow for three weeks to form peritoneal tumors.

For evaluation of ASC tumor tropism by BLI, 1×10^7 ASC-shCE2:nLuc cells were injected IP. At different time points, mice were anesthetized by isoflurane and injected IP with 0.1 mg/kg of furimazine (nLuc substrate) (Promega, WI, USA) and 150mg/kg of D-luciferin (GoldBio, MO, USA) dissolved in 100 μL sterile PBS. Mice were imaged to detect and measure bioluminescence signal intensity within 30 seconds of furimazine and five minutes of D-luciferin injections with acquisition times of 60 seconds. Bioluminescent images were captured using In Vivo MS FX PRO (Carestream Health, NY, USA) with 535nm filter (Acquisition time: 60 seconds) to eliminate spectral overlap. The fLuc substrate (D-luciferin) and nLuc substrate (furimazine) are enzyme specific and do not cross react. The results were analyzed using Bruker MI molecular imaging software.

To identify CD90+ ASCs in tumors, a single cell suspension of tumors was prepared. For this, mice were euthanized, the tumors removed and then transferred onto a Petri dish containing 10 ml of ice-cold PBS. Tumors were then minced (2 mm or less) and transferred into a 15 ml conical tube containing 10 ml of pre-warmed (37 °C) Dispase II (2.4 U/ml, Stem cell technologies, BC, Canada) in DMEM and incubated at 5% C02 and 37 °C for 30 min After incubation, the cell slurry was transferred onto a cell strainer (70 μm mesh) placed on top of a 50 ml conical tube and a gentle pressure was applied against the mesh using a syringe plunger. The flow-through cell suspension was collected in a 50 ml sterile conical tube and incubated with anti-CD90 primary (abeam, ab23894) and corresponding secondary antibodies (abeam, ab150113). Flow cytometry analysis was performed by using Beckman Coulter Gallios flow cytometer. IgG isotype (ab91353) was used as negative control. Data analysis was performed by using Kaluza® Flow analysis software (Beckman Coulter, Inc) and results are reported as the percentage of cells expressing CD90.

To study the co-localization of the ASCs with the peritoneal tumors by magnetic resonance imaging (MRI), OVASC-1 peritoneal tumors were implanted as mentioned above. Then, ASC-shCE2:nLuc cells were transfected with FluidMAG-D (150nm size) (Chemicell GmbH, Berlin, Germany) superparamagnetic iron oxide nanoparticles (SPION) to make ASC-shCE2:nLuc:SP. For that, 2×10^6 ASC-shCE2:nLuc cells were seeded in a 150 cm^2 Falcon™ tissue culture flask (Fisher Scientific, NH, USA) and treated with 162.5 μg/ml of FluidMAG-D for 24 hours. The ASC-shCE2:nLuc:SP cells were washed several times by PBS, harvested, and then injected (1×10^7 cells) into the peritoneum of tumor-bearing mice. The tropism of ASC-shCE2:nLuc:SP cells toward the OVASC-1-fLuc peritoneal tumors was evaluated by 1 Tesla ASPECT M2 MRI ten days post injection For MRI imaging, a 35mm mouse coil was used. The mouse was anesthetized by 1% isoflurane and then scanned using gradient echo with the external average (GRE EXT). The GRE EXT scans were performed with the following parameters: 24 slides at the coronal view, field of view 80×80 mm, slide thickness 1 mm with no gap between slides, sampling 256, encoding 256, time of echo 3.8ms, repetition time 15.4ms, and number of excitation 8. The captured images were converted to DICOM format and then evaluated by VivoQuant™ Software (Invicro, LLC).

To identify the locations of the ASC-shCE2:nLuc:SP cells inside the tumors by histochemistry, the mice were euthanized, the IP tumors removed, washed with 0.9% saline solution, placed inside a Cryomold (Fisher Scientific) filled with Tissue-Plus™ O.C.T compound (Fisher Scientific), and then snap frozen by liquid nitrogen The tumors were sectioned and then stained by using Gomori Iron Prussian Blue Stain (Newcomer Supply, WI). Photomicrography was conducted using a Leica microscope (10X - 60X objectives) and the slides were studied by a histopathologist at Biorepository and Histopathology Core Facility at Rutgers-CINJ.

For immunohistochemistry, tissue samples were prepared and incubated with anti-CD90 primary antibody (abeam, ab23894) for one hour at a dilution of 1:100. Tissues were then incubated with secondary antibody Goat anti-Mouse IgG Texas Red (Invitrogen) at a dilution of 1:1,000 for one hour in the dark followed by DAPI (Invitrogen, D1306) counterstain for 10 minutes. The slides were studied under a microscope at Rutgers Research Pathology Core Facility.

Evaluation of therapy response, ovarian cancer relapse and survival rate in nude mice

Female nude mice were injected with 5×10^6 of OVASC-1-fLuc cells to form intraperitoneal tumors as described above. The cancer cells were left to grow for 3 weeks to form tumors and the bioluminescence signal intensity reaches in the range of 1.0×10^8 to 1.0×10^9 (p/s) indicating presence of established tumors. Mice were then randomly divided into five groups of five and received treatment. Group 1 (G1) received vehicle only twice per week. The vehicle solution was composed of 1% cremophor:ethanol (50:50) and 99% saline (0.9%). Group 2 (G2) received cisplatin (5 mg/kg) plus paclitaxel (15 mg/kg) dissolved in vehicle once per week. Group 3 (G3) received irinotecan (40 mg/kg) twice per week (Thursdays and Saturdays) for ten weeks. Group 4 (G4) received irinotecan (80 mg/kg) twice per week (Thursdays and Saturdays) for ten weeks. Group 5 (G5) received ten million ASC-shCE2:nLuc cells once a week (Mondays) and irinotecan (40 mg/kg) twice per week (Thursdays and Saturdays) for ten weeks. In this protocol, the first drug dose was administered 72 hours post ASC injection and there was a 48 hours lag in between the first and second irinotecan injections. All drug and cell administrations were IP. To monitor disease progression and treatment effects, bioluminescence signal intensity was measured by using an IVIS Lumina III Imaging System (PerkinElmer, MA, USA) as previously described by our group [14]. The acquired images were analyzed by the Living Image 4.5 module. To eliminate spectral overlap, the BLI of fLuc and nLuc were performed on different days (two days apart).

Observable indicators of health (i.e, diarrhea, appetite, posture, movement) and body weight were continuously monitored to detect any treatment-related toxicities or disease-related morbidities resulting from the ascitic burden Loss of more than 10% body weight in one week or more than 20% at any time period was considered as the study end-point. When significant toxicity was observed, either the treatment was discontinued or mice were euthanized.

Tissue toxicity studies by hematology and histopathology

To evaluate the effects of treatment on mice blood factors, 50 μl blood samples were collected postmortem from mice in each group by cardiac puncture blood collection method and stored in BD Microtainer® blood collection tubes at room temperature. The samples were then tested for hematologic parameters by Element HT5 Veterinary Hematology Analyzer (Heska, CO, USA) at the In Vivo Research Services of Rutgers University.

To determine the toxicity to normal tissues inside the peritoneum after treatment, major organs in peritoneal cavity were removed immediately after the last treatment point. Organs were washed with saline, placed inside a Cryomold filled with Tissue-Plus™ O.C.T compound, and then snap frozen in liquid nitrogen Cryosectioning was performed at the Biospecimen Repository and Histopathology Service Core Facility at Rutgers-Cancer Institute of New Jersey followed by fixation and hematoxylin and eosin (H&E) staining. The slides were interpreted by a histopathologist at the Rutgers-Robert Wood Johnson University Hospital. Photomicrography was conducted using a Leica microscope (20X objective).

Statistical analysis

For in vitro studies, the experiments were repeated at least three times unless otherwise stated. Data are presented as mean ± SD (standard deviation). When two groups were compared, the statistical significance was determined by using Two-tailed Student's t-test. One-way analysis of variance (ANOVA) was used for multiple comparisons and Tukey's post hoc test was used for pairwise comparisons. Differences were considered statistically significant when p value was < 0.05.

Results

Assessment of the drug sensitivity and resistance of ovarian cancer cells

To assess the sensitivity of OVASC-1 ovarian cancer cells to prodrug metabolites, cell viability and clonogenic assays were performed. While the cell viability assay measured acute toxicity, the clonogenic assay evaluated all potential forms of cell death occurring after long-term exposure to anticancer drugs (chronic toxicity). In this experiment, 5-FU, 6-MP and SN-38, which are the toxic metabolites of 5-FC, 6-MPd, and irinotecan prodrugs, were examined [21–23]. Cisplatin was also used as a reference, as it is used as the standard-of-care for the treatment of ovarian cancer. For comparative purposes, established ovarian cancer cell lines representing low-grade ovarian cancer (i.e., SKOV-3 and A2780) and drug-resistant ovarian cancer (OVCAR-3 and A2780-Cis) were also investigated. The results of the cell viability assay show that OVASC-1 cells were the most drug-resistant and that SN-38 was the most potent cytotoxic drug of the ones tested (Table 1, Figure S1A–S1D). The IC50 of SN-38 fell within a low nanomolar range, whereas the IC_{50} of all the other drugs fell within the micromolar range. Of the established cell lines, OVCAR-3 and A2780-Cis showed more resistance to the drugs than the others. The IC_{50} values of cisplatin for OVASC-1 and A2780-Cis were 19.75 μM and 15.69 μM, respectively. This shows that OVASC-1 was more resistant to cisplatin than A2780-Cis. The results of the colony formation assay also show that SN-38 best prevented the formation of new colonies within

low nanomolar range (<20 nM) (Figure S2). All other drugs (i.e., 5-FU, 6-MP and cisplatin) were able to prevent the formation of colonies at micromolar levels (>10 μM).

To better understand the causes of OVASC-1 cells' drug resistance, they were characterized with an Aldehyde dehydrogenase (ALDH) enzyme activity assay and limiting dilution assay (LDA). ALDH plays a vital role in cellular detoxification and is upregulated in drug-resistant cells [24], Therefore, its measurement offers insight into resistance to therapy. The results of this experiment show that OVASC-1 cells present the highest percentage of ALDH $^{+}$ cells followed by OVCAR-3 (Figure 1A, Figure S3A) (*ANOVA, p<0.05). In addition, an LDA was performed to determine the frequency of CICs, also known as cancer stem-like cells (CSCs), which are able to initiate new colonies [2, 25]. The LDA shows that OVASC-1 presented the highest number of CICs in its population (~5%, 1 in 20) followed by OVCAR-3 cells (~3%, 1 in 32) (Figure 1B, Figure S3B).

To examine whether SN-38 can kill drug-resistant cells in OVASC-1 cell populations, we treated them with SN-38 and then measured the resulting change in the ALDH enzyme activity. We used cisplatin as a control for comparative purposes. The results of this study show that at low concentrations, both SN-38 and cisplatin first killed the sensitive cell population resulting in the enrichment of ALDH^{+} cells in the remaining population Once the drug concentration surpassed a certain threshold (i.e., 10 nM for SN-38 and 10 μM for cisplatin), the drug started to kill the drug-resistant cells (Figure 1C–1D) (*t-test, p<0.05).

Since OVASC-1 cells showed resistance to all four drugs tested in this study, we looked at the cell surface expression levels of MDR-1 and ABCG2 transporters. While various genetic and epigenetic factors may play roles in drug resistance, these two cell surface receptors are shared players in cancer cell adaptation to chemotherapy with cisplatin, SN-38, 5-FU and 6-MP [14, 26, 27]. The results of this experiment show that ~48% of the OVASC-1 cells exhibited an overexpression of MDR-1 while more than 93% of the population showed an overexpression of ABCG2 transporters on their surfaces (Figure 1E–1F, Figure S4–S5).

Evaluation of the sensitivity of OVASC-1 tumorspheres to SN-38

To examine the effectiveness at which SN-38 killed the CSCs in the OVASC-1 cell population, we cultured the cells under non-adherent conditions and generated CSC-rich tumorspheres (Figure 2A). To validate CSC enrichment, we measured the expression of typical stem cell biomarkers such as NANOG, SOX-2 and OCT-4 in OVASC-1 cells grown under both adherent and non-adherent conditions. The results of the experiment show a significant increase in stem cell biomarker expression in tumorspheres indicating CSC enrichment (Figure 2B) (*t-test, p<0.05). We also examined the expression levels of ABCG2 transporters in tumorspheres because ABCG2 is a biomarker for ovarian CSCs [28]. The results of the experiment show a significant increase in the density of ABCG2 transporters on the surface of OVASC-1 cells in tumorspheres relative to OVASC-1 cells grown under adherent conditions. While the percentage of cells that expressed ABCG2 remained the same for OVASC-1 cells grown under adherent and non-adherent conditions, the X-mean (Mean Fluorescence Intensity) for ABCG2 expression on the surface of OVASC-1 tumorspheres (i.e., X-Mean: 44.04) showed a 2-fold increase in comparison to those of cells grown under adherent conditions (i.e., X-Mean: 21.7) (Figure 2C vs. 1F, and Figure S5 vs.

S6). Since MDR-1 is not a biomarker for ovarian CSCs, we also measured its expression in OVASC-1 tumorspheres as a control. The results of this experiment show that the density of MDR1 expression on the surfaces of OVASC-1 tumorspheres was similar to that of OVASC-1 cells grown under adherent conditions (Figure 2D vs. Figure 1E, and Figure S4 vs. Figure S7). Next, we treated the tumorspheres with different concentrations of SN-38 to determine its ability to kill the CSC-rich tumorspheres. The results of this experiment show that the drug was able to kill cancer cells in the tumorspheres as evidenced by a significant reduction in their diameters (Figure 2E) (*t-test, $p<0.05$). While SN-38 at concentration of 100 nM could completely kill the OVASC-1 tumorspheres, cisplatin could achieve approximately the same level of tumorsphere killing efficiency at concentration of 100 μM. To examine whether remaining cells in the treated tumorspheres were alive or dead, we stained them with calcein AM (C-AM) and propidium iodide (PI) to visualize the live and dead cells, respectively. The results show that remaining cells in the SN-38- (100 nM) and cisplatin-treated (100 μM) groups were in fact clumps of cell debris (Figure 2F). Tumorspheres treated with lower concentrations of drugs included a mixture of live and dead cells (Figure S8).

Evaluation of the functionality of the genetically engineered ASCs

An ASC clone that stably expressed shCE2 and nanoluciferase genes (ASC-shCE2:nLuc) was genetically engineered to allow for simultaneous disease therapy and in vivo imaging (Figure S9A). To examine whether functional shCE2 was in fact secreted outside of the ASCs, two experiments were performed. First, the activity of the carboxylesterase enzyme secreted into the culture media was examined by removing the media in which the ASC-shCE2:nLuc cells were grown and through treatment with FDA (CE2 substrate and nonfluorescent). The kinetics of FDA conversion into its fluorescently active byproduct fluorescein was then measured. The results of this experiment show that the fluorescence of media continuously increased over time, revealing the activity of shCE2. Relative to the fluorescent intensity of the culture media never put in contact with cells, an almost 8 fold (81.88/10.74) increase in the rate of FDA conversion was observed for the media in which ASC-shCE2:nLuc cells were grown (Figure S9B). In contrast, the culture media of the ASC-hCE2:nLuc cells (nonsecretory CE2) did not show any significant changes in fluorescent intensity, indicating inefficiency in FDA conversion We also examined the capacity for the secreted shCE2 in the culture media to convert irinotecan into SN38. For this purpose, we removed the culture media in which ASC-shCE2:nLuc cells were grown and then treated it with irinotecan. The culture media was then analyzed by LC/MS to identify corresponding irinotecan and SN-38 ion fragments. The results of this experiment show that shCE2 secreted from ASC-shCE2:nLuc cells converted a portion of the irinotecan prodrug into SN-38 (Figure S9C–S9D). The two experiments validate that the ASC-shCE2:nLuc cells secrete an active form of shCE2 into culture media with the ability to convert irinotecan into SN-38. We also examined the activity of the nanoluciferase in ASC-shCE2:nLuc cells by incubating them with enzyme substrate furimazine. A clone of ASC-shCE2:nLuc cells with the highest expression of both shCE2 and nanoluciferase genes was isolated (Figure S10). We then performed an experiment to assess whether the isolated ASC-shCE2:nLuc clone in combination with irinotecan could generate sufficiently high concentrations of SN-38 lethal to OVASC-1 cells. For this purpose, we first determined the maximum concentration of

irinotecan that can be used in cell culture media without being toxic to ASCs or OVASC-1 cells. The results of this experiment show that irinotecan at a 1 μM concentration was not toxic to either group of cells (Figure S11A–S11B). Then, ASC-shCE2:nLuc and OVASC-1 cells were cocultured and treated with irinotecan (1 μM). The results of this experiment show a significant reduction in the viability of the OVASC-1 cells cocultured with ASC-shCE2:nLuc cells and treated with irinotecan (1 μM) (Figure S11C).

Evaluation of the tumor tropism of the engineered ASCs by BLI, MRI and immuno/histochemistry

To study the tropism of the ASC-shCE2:nLuc cells, we first injected the cells into the peritoneum of a nude mouse (without tumors) and tracked the cells by BLI. The intention was to study the late of the ASC-shCE2:nLuc cells in mouse peritoneum The results of the experiment show that most of the ASCs disappeared from the field of view and were not detectable after two weeks. However, long-term imaging tests detected bioluminescence signals from two locations within the mouse body after seven weeks (Figure S12A–12B). To investigate further, the mouse was euthanized, and the luminescent area removed, stained and studied under a microscope. The histopathology results show that the luminescent area included an aggregate of ASCs in mesentery without evidence of malignancy (Figure S12C).

We then performed experiments to assess the tumor tropism of the engineered ASC-shCE2:nLuc cells. For this purpose, OVASC-1 cells that stably expressed the firefly luciferase gene (OVASC-fLuc) were genetically engineered. OVASC-fLuc cells were then injected IP and were left to grow for three weeks to provide ample time for the tumors to establish and metastasize (Figure S12D). Three weeks after tumor establishment, the ASC-shCE2:nLuc cells were injected IP and their distribution and migration was tracked by BLI. Since firefly luciferase and nanoluciferase substrates do not cross-react, they could be imaged without interference. The BLI data show that the ASC-shCE2:nLuc cells colocalized with OVASC-fLuc cells as soon as three days postinjection (Figure 3A). On day 11, the mouse was euthanized, the tumors removed and imaged in the presence of furimazine (nLuc substrate). The results of this experiment showed the existence of nLuc enzyme within the dissected tumors indicating the presence of ASC-shCE2nLuc cells (Figure 3A). We then prepared a suspension of single cells from the extracted tumors and studied them for CD90 biomarker expression CD90 is a typical biomarker expressed on the surface of ASCs [29], but not on OVASC-1 cells (Figure S13). The results of this experiment showed that approximately 5% of the analyzed cells were CD90+ (Figure 3B). Using cell sorting, we separated the CD90+ cells and transferred them into a well followed by addition of furimazine. The results of this experiment showed that the CD90+ cells had nLuc expression whereas the $CD90^{-}$ cells did not (Figure 3B).

To examine the localization of the ASC-shCE2:nLuc cells within tumors at a higher resolution and to determine potential applications of this approach in clinical settings, we treated the ASC-shCE2:nLuc cells with SPIONs at a non-toxic concentration to form ASC-shCE2:nLuc-SP cells (Figure S14). Since the cells were loaded with SPIONs, they could be detected by T2*-weighted MRI sequence. The MRI data revealed the areas within the peritoneum in which ASC-shCE2:nLuc-SP cells were localized (Figure 3C). Using the MR

images as a guide, a cluster of tumors with blackened surfaces was detected under the liver after tissue dissection (Figure 3D).

Furthermore, the presence of SPION nanoparticles in the ASCs made it possible to identify the exact locations of the ASCs within the tumors by iron-staining and immuno/histochemistry. The histochemistry of the dissected tumors shows that the ASC-shCE2:nLuc-SP cells were localized in both tumor stroma and necrotic regions (Figure 4A–4B). The staining of the tumor tissue sections with CD90 antibody confirmed the presence of ASCs inside the tumor tissues (Figure 4A–4B). A higher magnification of the H&E stained tumor tissue section clearly showed presence of iron in cells with vacuolated cytoplasm consistent with adipocytes (Figure 4C).

Evaluation of ovarian cancer progression, responses to therapy and prevention of relapse

To determine the efficacy of the engineered ASCs in treating metastatic drug-resistant ovarian cancer, suicide gene expressing ASC-shCE2:nLuc cells were used in combination with irinotecan OVASC-1-fLuc cells were injected into the peritoneum of nude mice to establish tumors. After three weeks, the change in tumor mass in peritoneum was measured by BLI to confirm the establishment of tumors and of advanced disease. The mice were then divided into five groups (G1 to G5) of five and given treatments as delineated in Table 2. The analysis of images of mice in G1 illustrated a steady-state enhancement in the bioluminescence signal, denoting an increase in tumor mass over time (Figure S15A–S15B). The animals in this group were either euthanized (~7 weeks after tumor implantation) due to significant weight loss or died due to disease progression into vital organs (Table 2, Figure S15C). Mice in G2 received standard-of-care cisplatin/PTX using a regimen based on previously published reports [30, 31]. The mice in this group did not respond to the standard-of-care therapy, as tumor masses did not significantly decrease over the treatment period. The mice in this group were euthanized due to disease progression and the development of bulky ascites after ~8 weeks (Table 2, Figure 5A–5B, Figure S16). Mice in G3 received a therapeutic dose of irinotecan (40 mg/kg) because it is close to the equivalent dose used in humans and following previously published preclinical studies of mice [32, 33]. One mouse in this group showed a complete response without any relapse, whereas one mouse showed no response at all. The three remaining mice in this group showed a partial response. All mice that responded to therapy remained healthy and did not show any gastrointestinal (GI)-related toxicity as evidenced by the absence of weight loss, diarrhea and loss of appetite during the treatment period. Post treatment, mice were euthanized when they showed signs of disease progression into vital organs, including significant weight loss and/or the formation of bulky ascites and interference with normal functions (Table 2, Figure 5C–5D, Figure S17). An analysis of ABCG2 transporters on the surfaces of OVASC-1 cells extracted from nonresponsive tumors in this group showed a significant upregulation of the said transporter (Figure S18). Mice in G4 received irinotecan (80 mg/kg) where three mice in this group showed a complete response and two exhibited a partial response. The two mice that partially responded and the one mouse with the complete response experienced significant weight variations, frequent diarrhea, low levels of activity, and a loss of appetite during the treatment period, suggesting the manifestation of GI-related toxicity. Mice in this group were euthanized either due to significant and rapid weight loss or formation of bulky

ascites (Table 2, Figure 5E–5F, Figure S19). Mice in G5 were treated with ASC-shCE2:nLuc cells and irinotecan (40 mg/kg). The bioluminescent intensities of OVASC-1-fLuc tumors (firefly luciferase) and ASC-shCE2:nLuc cells (nanoluciferase) were measured and data related to each mouse analyzed. A quantitative analysis of bioluminescence levels of ASC-shCE2:nLuc cells measured before and after irinotecan injection shows that the ASC cells responded to the prodrug as evidenced by a significant change in signal intensity (Figure S20). Four mice in this group showed a complete response to therapy, remained healthy during the treatment period and did not show any signs of GI-related toxicity. Furthermore, we did not detect any bioluminescent signals even four weeks after the last day of therapy. One mouse in this group showed a more than 90% response to therapy but the residual tumor was still detectable on the last day of therapy and relapsed when the therapy stopped (Table 2, Figure 5G–5H, Figure S21). The relapsed tumor in this mouse was found to be the result of metastasis to regions outside of the peritoneum postmortem.

The statistical analysis of bioluminescent signal intensity levels among groups (ANOVA, Post hoc Tukey test, $*p<0.05$) in conjunction with the Kaplan-Meier Survival Estimator show that the treatment of mice bearing drug-resistant intraperitoneal tumors with cisplatin +PTX neither reduced the tumor mass ($p=0.78$) nor provided a survival benefit (0% survival rate) (Figure 6A–6B, Figure S22). Data analysis also shows that relative to cisplatin+PTX treated group, the treatment of mice with irinotecan 40 mg/kg ($p=0.021$) and irinotecan 80 mg/kg ($p=0.0005$) significantly reduced tumor masses and increased survival rates by 20% and 40%, respectively (Figure 6A–6B, Figure S22). The observed 80% death in G3 (irinotecan 40 mg/kg) occurring after treatment was due to disease progression, the formation of bulky ascites and interference with normal vital organs' functions. In contrast, the observed 60% death in G4 (irinotecan 80 mg/kg) occurring during the treatment period, was mainly due to toxicity to the GI tract. Overall, the treatment of mice with ASC-shCE2:nLuc plus irinotecan (40 mg/kg) was found to be the most effective in reducing the tumor burden ($p=0.000043$), delivering complete responses and increasing survival rates in 80% of the mice without any observable treatment-related toxicity (Figure 6A–6B, Figure S22).

Evaluation of tissue toxicity by histopathology and hematology

The monitoring of weight over the treatment period shows that mice in G2, G3 and G5 tolerated the therapy as evidenced by negligible negative impacts on weight changes (Figure S15–S21). However, the mice in G4 treated with irinotecan (80 mg/kg) exhibited significant weight variations, a loss of appetite, lethargy and frequent diarrhea. To investigate whether any toxicity occurred at the cellular level, we applied histopathological methods to major peritoneal organs. An analysis of tissue slides did not reveal any notable toxicity to the peritoneal organs of mice in any group (Figure 7). Furthermore, we analyzed mice blood (hematology) because neutropenia is one of the hematological toxicities (rare) reported in patients treated with irinotecan. The results show that mice in all groups tolerated the therapy and that there was no significant change to any of the blood factors (Figure S23).

Discussion

As a first step toward achieving our objectives, we obtained OVASC-1 cells from a patient with recurrent ovarian cancer and used them as a drug-resistant model in this study. To validate the resistance of this model to chemotherapeutics and to identify an effective enzyme/prodrug system for its treatment, we treated OVASC-1 cells with cisplatin, 5-FU, SN-38 and 6-MP. The results of cell viability and clonogenic assays showed that OVASC-1 cells were highly resistant to cisplatin and even more so than A2780-Cis as well as to the prodrug metabolites. The only drug that could kill the OVASC-1 cells within a low nanomolar range was SN-38. Based on this outcome and given that the potency of prodrug metabolites plays an important role in the anticancer efficacy of enzyme/prodrug systems, we selected CE2/ irinotecan as the most suitable one for the subsequent in vivo studies. To identify factors contributing to OVASC-1 cell resistance to chemotherapy, we measured percentages of ALDH+ cells and CICs (CSCs) as these two cell populations have been shown to be key players in imparting drug resistance. Interestingly, the LDA showed that almost 5% of the cell population exhibited stem-like characteristics with the ability to self-renew and generate new colonies. Although published data with established cell lines show that usually less than 2% of cancer cell populations are CSCs [34], it was curious to observe that approximately 5% of the OVASC-1 cells had stem-like characteristics. From our data and similar observations by other groups [35, 36], it appears that donor's (patient) treatment with chemotherapeutics may have led to enrichment in CSC populations. While cancer cells develop resistance against anticancer drugs through a variety of different mechanisms [37], overall it appears that the presence of high percentages of ALDH+ cells, CSCs, and MDR-1/ ABCG2 positive cells are among the main factors contributing to OVASC-1 cell drug resistance.

As a next step, we characterized OVASC-1 cells as tumorspheres because almost all ovarian cancer patients have ascites at recurrence with leaked cancer cells into the peritoneum and existing as spheroids (tumorspheres). The significance of tumorspheres lies in their exhibiting cancer stem-like phenotypes and the capacity for distal metastatic spread [38]. Our OVASC-1 tumorsphere characterization studies show that they are enriched with CSCs with significantly high expressions of ABCG2 transporters. Since ABCG2 transporters are responsible for resistance to SN-38 [27, 39], we examined whether the selection of SN-38 as the most effective prodrug metabolite used in this study was also effective against tumorspheres. We observed that SN-38 can eradicate OVASC-1 tumorspheres as long as they are exposed to at least 100 nM of the drug. While this is exciting, achieving this drug concentration within tumors may be difficult through systemic chemotherapy, as many patients may not be able tolerate the associated cytotoxicity to normal tissues. To address this dilemma, we hypothesized that by using MSCs that express shCE2 enzyme and in combination with irinotecan, high concentrations of SN-38 can be targeted and delivered to tumors killing OVASC-1 drug-resistant cells but without toxicity to normal tissues. It is noteworthy that SN-38 is approximately 1000 fold more potent than its prodrug irinotecan [40]. MSCs are known to be recruited to sites of wound healing and growing tumors (wounds that do not heal) due to their repair functions [41–43]. The migration and extravasation of mesenchymal stem cells into a tumor tissue involves an active process

driven by tumor-secreted cytokines [44]. This characteristic of MSCs is currently being exploited in both preclinical and clinical studies to develop more effective and less toxic treatments for different types of cancer [45–47] (clinicaltrials.gov, and). To test the hypothesis, we genetically engineered a clone of ASCs that stably expressed both shCE2 and nanoluciferase genes (ASC-shCE2:nLuc). The expression and functionality of both enzymes were confirmed via an enzyme activity assay, LC/MS and a cell toxicity assay. We then examined whether the genetically engineered ASCs could migrate toward ovarian peritoneal tumors after IP injection The live cell tracking study shows that in the absence of intraperitoneal tumors, ASCs tend to migrate toward mesentery (ASC niche) after IP injection This observation is consistent with past reports on the fate of MSCs after intraperitoneal administration [48]. However, in the presence of intraperitoneal tumors the ASCs colocalized with cancer cells as soon as three days post injection SPION-loaded ASCs also afforded us the opportunity to locate ASCs within the peritoneum by MRI at a higher resolution From the MRI images we identified hot spots otherwise hidden from human eyes. Using MRI results as a guide, we dissected the mouse abdomen and detected several tumors hidden under the liver. Interestingly, the presence of SPION-loaded ASCs in tumors made it possible for us to detect them easily owing to their blackened surfaces. This suggests that engineered SPION-loaded ASCs can be used by surgeons to accurately mark sites of metastasis by MRI and to then perform more successful debulking surgery procedures given the tumors' darkened surfaces. Most importantly, the immune/histochemistry of tumor tissues showed a localization of ASCs in both tumor stroma and necrotic regions, providing a unique opportunity to deliver therapeutics to not only the tumor stroma in which the tumor supporting cells such as fibroblasts and tumor-associated macrophages reside, but also to necrotic and hypoxic regions in which the CSCs reside [49,50].

Our in vivo data show that the treatment of OVASC-1 tumors with cisplatin and PTX did not result in a statistically significant therapy response. Since the OVASC-1 cells were isolated from a patient with recurrent drug-resistant disease, this response rate was expected. In contrast, mice treated with 40 mg/kg of irinotecan showed a significant response to therapy although the survival benefit was marginal (20%). This survival rate is in agreement with clinical outcomes of ovarian cancer therapy using irinotecan, which has survival benefits of 10% to 30% [13]. These results also indicate that a 40 mg/kg drug concentration is sufficient in killing mostly the drug-sensitive cell populations and with negligible drug-related toxicity during the treatment period. However, this drug dose was inadequate in killing the drug-resistant cell population, as 4/5 mice exhibited a partial response followed by cancer relapse. An analysis of ABCG2 transporter expression in nonresponsive mice in this group showed a significant upregulation of this transporter. This result is consistent with published data denoting ABCG2 as a major source of cancer resistance to therapy with irinotecan /SN-38 [14, 27, 39]. As a next step, we doubled the drug dose to 80 mg/kg to push the limits close to the maximum tolerating dose to examine the possibility of obtaining a superior therapy response [51]. While we observed a more significant response to therapy (3 mice were cured), unfortunately one of the cured mice died and two others with partial responses also showed severe signs of drug-related toxicity such as frequent diarrhea and significant body weight loss. Although treatment with higher concentrations of irinotecan cured more mice of the disease, it also led to higher rates of treatment-related mortality. To limit toxicity to the

tumors and to preserve healthy tissues, we treated another group of mice with ASC-shCE2:nLuc cells in combination with the safe irinotecan dose (i.e., 40 mg/kg). The dosing regimen was scheduled such that the first drug dose was administered 72 hours after ASC injection This was adopted to leave ample time for the ASCs to migrate to tumors, colocalize with cancer cells and secrete high concentrations of CE2. In addition, rather than providing a bolus dose, the irinotecan was injected in two separate smaller doses to minimize drug-related toxicity. Based on our preliminary studies we also found that leaving 48 hours of lag time in between the first and second dose of irinotecan is more effective than daily administration The outcomes of this therapeutic protocol show that mice in this group responded fully to the therapy without any signs of toxicity. In fact, 4/5 mice in this group remained cancer free for at least six weeks post treatment and did not show any signs of cancer relapse or toxicity to normal tissues. Overall, the data show that shCE2-expressing ASCs applied in combination with irinotecan can kill drug-resistant OVASC-1 tumors more effectively than applying irinotecan alone or cisplatin+PTX. Regarding the safety of this approach, hematology and histopathology results show that the toxic effects of therapy were limited to tumor tissues, as we could not detect any negative impacts on blood factors (e.g., neutropenia and leukopenia) or on major intraperitoneal organs. In the clinic, major forms of nonhematological toxicity that interrupt cancer therapy with irinotecan are GI-related and echo what we observed in G4 (e.g., diarrhea, vomiting, edema, etc.) [13]. Overall, our toxicity data in combination with efficacy outcomes reveal a very promising nonsurgical approach to overcoming drug resistance in recurrent metastatic ovarian cancer.

Conclusions

Two ongoing clinical trials on the use of stem cells for the targeted therapy of ovarian cancer are currently underway (and) setting the stage for future stem cell-mediated therapeutics. Our data show that SN-38 is more effective as a prodrug metabolite than 5-FU and 6-MP. Therefore, CE2/irinotecan was used as the most effective enzyme/prodrug system for killing drug-sensitive and resistant ovarian cancer cells. As the data presented in this work showed a complete tumor response and imparted survival benefits in 80% of the subjects, stem cell-mediated suicide gene therapy delivered through the shCE2/irinotecan system appears to constitute an effective nonsurgical means of treating recurrent ovarian cancer with intraperitoneal metastasis. The developed stem cell-mediated tumor-selective approach has the potential to be used for the treatment of other cancers of peritoneal cavity, such as those of the liver, pancreas, stomach, kidneys and colon

Supplementary Material

Refer to Web version on PubMed Central for supplementary material.

Acknowledgments

This work was supported by a grant from the NIH/NCI (R01CA175318). This work was also supported in part by the NIH/NCI Flow Cytometry (P30CA072720–5924) and Biorepository and Histopathology (P30CA072720–5919) Shared Resources of the Rutgers-Cancer Institute of New Jersey (NCI-designated Comprehensive Cancer Center).

References

[1]. Marth C, Reimer D, Zeimet AG, Front-line therapy of advanced epithelial ovarian cancer: standard treatment, Ann Oncol, 28 (2017) viii36–viii39. [PubMed: 29232473]

[2]. Shah MM, Landen CN, Ovarian cancer stem cells: are they real and why are they important?, Gynecol Oncol, 132(2014)483–489. [PubMed: 24321398]

[3]. Miyoshi Y, Ueda Y, Morimoto A, Yokoyama T, Matsuzaki S, Kobayashi E, Kimura T, Yoshino K, Fujita M, Enomoto T, Kimura T, Salvage chemotherapy for ovarian carcinoma recurring during or after consolidation chemotherapy with paclitaxel, Anticancer research, 31 (2011)4613–4617. [PubMed: 22199338]

[4]. Hjortkjaer M, Kanstrup H, Jakobsen A, Steffensen KD, Veliparib and topotecan for patients with platinum-resistant or partially platinum-sensitive relapse of epithelial ovarian cancer with BRCA negative or unknown BRCA status, Cancer Treat Res Commun, 14 (2018) 7–12. [PubMed: 30104007]

[5]. Chekerov R, Hilpert F, Mahner S, El-Balat A, Harter P, De Gregorio N, Fridrich C, Markmann S, Potenberg J, Lorenz R, Oskay-Oezcelik G, Schmidt M, Krabisch P, Lueck HJ, Richter R, Braicu EI, du Bois A, Sehouli J, Noggo AT Investigators, Sorafenib plus topotecan versus placebo plus topotecan for platinum-resistant ovarian cancer (TRIAS): a multicentre, randomised, double-blind, placebo-controlled, phase 2 trial, Lancet Oncol, 19 (2018)1247–1258. [PubMed: 30100379]

[6]. Bodurka DC, Levenback C, Wolf JK, Gano J, Wharton JT, Kavanagh JJ, Gershenson DM, Phase II trial of irinotecan in patients with metastatic epithelial ovarian cancer or peritoneal cancer, J Clin Oncol, 21 (2003)291–297. [PubMed: 12525521]

[7]. Yoshino K, Kamiura S, Yokoi T, Nakae R, Fujita M, Takemura M, Adachi K, Wakimoto A, Nishizaki T, Shiki Y, Tsutsui T, Kanda Y, Kobayashi E, Hashimoto K, Mabuchi S, Ueda Y, Sawada K, Tomimatsu T, Kimura T, Combination chemotherapy with irinotecan and gemeitabine for taxane/pktinum-resistant/refractory ovarian and primary peritoneal cancer: a multicenter phase I/II trial (GOGO-Ov6), Cancer Chemother Pharmacol, 80 (2017) 1239–1247. [PubMed: 29080971]

[8]. Gordon AN, Granai CO, Rose PG, Hainsworth J, Lopez A, Weissman C, Rosales R, Sharpington T, Phase II study of liposomal doxorubicin in platinum- and paclitaxel-refractory epithelial ovarian cancer, J Clin Oncol, 18 (2000) 3093–3100. [PubMed: 10963637]

[9]. Shoji T, Takatori E, Omi H, Kagabu M, Honda T, Futagami M, Yokoyama Y, Kaiho M, Tokunaga H, Otsuki T, Takano T, Yaegashi N, Kojimahara T, Ohta T, Nagase S, Soeda S, Watanebe T, Nishiyama H, Sugiyama T, A phase II study of irinotecan and pegylated liposomal doxorubicin in platinum-resistant recurrent ovarian cancer (Tohoku Gynecologic Cancer Unit 104 study), Cancer Chemother Pharmacol, 80(2017)355–361. [PubMed: 28656383]

[10]. Shin W, Lee HJ, Yang SJ, Paik ES, Choi HJ, Kim TJ, Choi CH, Lee JW, Bae DS, Kim BG, Retrospective study of combination chemotherapy with etoposide and ifosfamide in patients with heavily pretreated recurrent or persistent epithelial ovarian cancer, Obstet Gynecol Sci, 61 (2018) 352–358. [PubMed: 29780777]

[11]. Bozkaya Y, Dogan M, Umut Erdem G, Tulunay G, Uncu H, Arik Z, Demirci U, Yazici O, Zengin N, Effectiveness of low-dose oral etoposide treatment in patients with recurrent and platinum-resistant epithelial ovarian cancer, J Obstet Gynaecol, 37 (2017) 649–654. [PubMed: 28325092]

[12]. Markman M, Webster K, Zanotti K, Kulp B, Peterson G, Belinson J, Phase 2 trial of single-agent gemeitabine in platinum-paclitaxel refractory ovarian cancer, Gynecol Oncol, 90 (2003) 593–596. [PubMed: 13678730]

[13]. Matsumoto K, Katsumata N, Yamanaka Y, Yonemori K, Kohno T, Shimizu C, Andoh M, Fujiwara Y, The safety and efficacy of the weekly dosing of irinotecan for platinum-and taxanes-resistant epithelial ovarian cancer, Gynecol Oncol, 100(2006)412–416. [PubMed: 16298422]

[14]. Sarkar S, Malekshah OM, Nomani A, Patel N, Hatefi A, A novel chemotherapeutic protocol for peritoneal metastasis and inhibition of relapse in drug resistant ovarian cancer, Cancer Med, 7 (2018) 3630–3641. [PubMed: 29926538]

[15]. Ponte AL, Marais E, Gallay N, Langonne A, Delorme B, Herault O, Charbord P, Domenech J, The in vitro migration capacity of human bone marrow mesenchymal stem cells: comparison of

chemokine and growth factor chemotactic activities, Stem Cells, 25 (2007) 1737–1745. [PubMed: 17395768]

[16]. Hatfield JM, Wierdl M, Wadkins RM, Potter PM, Modifications of human carboxylesterase for improved prodrug activation, Expert Opin Drug Metab Toxicol, 4 (2008) 1153–1165. [PubMed: 18721110]

[17]. Ma MK, McLeod HL, Lessons learned from the irinotecan metabolic pathway, Curr Med Chem, 10(2003) 41–49. [PubMed: 12570720]

[18]. Kidd S, Spaeth E, Dembinski JL, Dietrich M, Watson K, Klopp A, Battula VL, Weil M, Andreeff M, Marini FC, Direct evidence of mesenchymal stem cell tropism for tumor and wounding microenvironments using in vivo bioluminescent imaging, Stem Cells, 27 (2009) 2614–2623. [PubMed: 19650040]

[19]. Ayen A, Jimenez Martinez Y, Marchal JA, Boulaiz H, Recent Progress in Gene Therapy for Ovarian Cancer, Int J Mol Sci, 19 (2018).

[20]. Hu Y, Smyth GK, ELDA: extreme limiting dilution analysis for comparing depleted and enriched populations in stem cell and other assays, J Immunol Methods, 347 (2009) 70–78. [PubMed: 19567251]

[21]. Karjoo Z, Chen X, Hatefi A, Progress and problems with the use of suicide genes for targeted cancer therapy, Adv Drug Deliv Rev, 99 (2016) 113–128. [PubMed: 26004498]

[22]. Malekshah OM, Chen X, Nomani A Sarkar S, Hatefi A, Enzyme/Prodrug Systems for Cancer Gene Therapy, Current pharmacology reports, 2 (2016) 299–308. [PubMed: 28042530]

[23]. Nouri FS, Wang X, Hatefi A, Genetically engineered theranostic mesenchymal stem cells for the evaluation of the anticancer efficacy of enzyme/prodrug systems, J Control Release, 200 (2015) 179–187. [PubMed: 25575867]

[24]. Januchowski R, Wojtowicz K, Sterzyska K, Sosiska P, Andrzejewska M, Zawierucha P, Nowicki M, Zabel M, Inhibition of ALDH1A1 activity decreases expression of drug transporters and reduces chemotherapy resistance in ovarian cancer cell lines, Int J Biochem Cell Biol, 78 (2016)248–259. [PubMed: 27443528]

[25]. Burgos-Ojeda D, Rueda BR, Buckanovich RJ, Ovarian cancer stem cell markers: prognostic and therapeutic implications, Cancer letters, 322(2012) 1–7. [PubMed: 22334034]

[26]. Di Nicolantonio F, Mercer SJ, Knight LA, Gabriel FG, Whitehouse PA, Sharma S, Fernando A, Glaysher S, Di Palma S, Johnson P, Somers SS, Toh S, Higgins B, Lamont A, Gulliford T, Hurren J, Yiangou C, Cree IA, Cancer cell adaptation to chemotherapy, BMC Cancer, 5 (2005) 78. [PubMed: 16026610]

[27]. Jandu H, Aluzaite K, Fogh L, Thrane SW, Noer JB, Proszek J, Do KN, Hansen SN, Damsgaard B, Nielsen SL, Stougaard M, Knudsen BR, Moreira J, Hamerlik P, Gajjar M, Smid M, Martens J, Foekens J, Pommier Y, Brunner N, Schrohl AS, Stenvang J, Molecular characterization of irinotecan (SN-38) resistant human breast cancer cell lines, BMC Cancer, 16 (2016) 34. [PubMed: 26801902]

[28]. Dou J, Jiang C, Wang J, Zhang X, Zhao F, Hu W, He X, Li X, Zou D, Gu N, Using ABCG2-molecule-expressing side population cells to identify cancer stem-like cells in a human ovarian cell line, Cell Biol Int, 35 (2011) 227–234. [PubMed: 21108606]

[29]. Mildmay-White A, Khan W, Cell Surface Markers on Adipose-Derived Stem Cells: A Systematic Review, Curr Stem Cell Res Ther, 12 (2017) 484–492. [PubMed: 27133085]

[30]. Aston WJ, Hope DE, Nowak AK, Robinson BW, Lake RA, Lesterhuis WJ, A systematic investigation of the maximum tolerated dose of cytotoxic chemotherapy with and without supportive care in mice, BMC Cancer, 17 (2017) 684. [PubMed: 29037232]

[31]. Helland O, Popa M, Vintermyr OK, Molven A, Gjertsen BT, Bjorge L, McCormack E, First in-mouse development and application of a surgically relevant xenograft model of ovarian carcinoma, PloS one, 9 (2014) e89527. [PubMed: 24594904]

[32]. Gutova M, Shackleford GM, Khankaldyyan V, Herrmann KA, Shi XH, Mittelholtz K, Abramyants Y, Blanchard MS, Kim SU, Annala AJ, Najbauer J, Synold TW, D'Apuzzo M, Barish ME, Moats RA, Aboody KS, Neural stem cell-mediated CE/CPT-11 enzyme/prodrug therapy in transgenic mouse model of intracerebellar medulloblastoma, Gene therapy, 20 (2013) 143–150. [PubMed: 22402322]

[33]. Choi MK Ahn BJ, Yim DS, Park YS, Kim S, Sohn TS, Noh JH, Heo JS, Lee J, Park SH, Park JO, Lim HY, Kang WK, Phase I study of intraperitoneal irinotecan in patients with gastric adenocarcinoma with peritoneal seeding, Cancer Chemother Pharmacol 67 (2011)5–11. [PubMed: 20213078]

[34]. Enderling H, Hlatky L, Hahnfeldt P, Cancer Stem Cells: A Minor Cancer Subpopulation that Redefines Global Cancer Features, Front Oncol, 3 (2013) 76. [PubMed: 23596563]

[35]. Kakar SS, Ratajczak MZ, Powell KS, Moghadamfalahi M, Miller DM, Batra SK, Singh SK, Withaferin a alone and in combination with cisplatin suppresses growth and metastasis of ovarian cancer by targeting putative cancer stem cells, PloS one, 9 (2014) e107596. [PubMed: 25264898]

[36]. Rich JN, Cancer stem cells: understanding tumor hierarchy and heterogeneity, Medicine (Baltimore), 95 (2016) S2–7. [PubMed: 27611934]

[37]. Ahmed N, Abubaker K, Findlay JK, Ovarian cancer stem cells: Molecular concepts and relevance as therapeutic targets, Molecular aspects of medicine, 39(2014) 110–125. [PubMed: 23811037]

[38]. Ahmed N, Stenvers KL, Getting to know ovarian cancer ascites: opportunities for targeted therapy-based translational research, Front Oncol, 3 (2013) 256. [PubMed: 24093089]

[39]. Tuy HD, Shiomi H, Mukaisho KI, Naka S, Shimizu T, Sonoda H, Mekata E, Endo Y, Kurumi Y, Sugihara H, Tani TM. Tani, ABCG2 expression in colorectal adenocarcinomas may predict resistance to irinotecan, Oncology letters, 12 (2016) 2752–2760. [PubMed: 27698852]

[40]. Danks MK, Morton CL, Krull EJ, Cheshire PJ, Richmond LB, Naeve CW, Pawlik CA, Houghton PJ, Potter PM, Comparison of activation of CPT-11 by rabbit and human carboxylesterases for use in enzyme/prodrug therapy, Clin Cancer Res, 5 (1999) 917–924. [PubMed: 10213229]

[41]. Dvorak HF, Tumors: wounds that do not heal Similarities between tumor stroma generation and wound healing, N Engl J Med, 315 (1986) 1650–1659. [PubMed: 3537791]

[42]. Gutova M, Najbauer J, Frank RT, Kendall SE, Gevorgyan A, Metz MZ, Guevorkian M, Edmiston M, Zhao D, Glackin CA, Kim SU, Aboody KS, Urokinase plasminogen activator and urokinase plasminogen activator receptor mediate human stem cell tropism to malignant solid tumors, Stem Cells, 26(2008) 1406–1413. [PubMed: 18403751]

[43]. Shi M, Li J, Liao L, Chen B, Li B, Chen L, Jia H, Zhao RC, Regulation of CXCR4 expression in human mesenchymal stem cells by cytokine treatment: role in homing efficiency in NOD/SCID mice, Haematologica, 92 (2007) 897–904. [PubMed: 17606439]

[44]. Teo GS, Ankrum JA, Martinelli R, Boetto SE, Simms K, Sciuto TE, Dvorak AM, Karp JM, Carman CV, Mesenchymal stem cells transmigrate between and directly through tumor necrosis factor-alpha-activated endothelial cells via both leukocyte-like and novel mechanisms, Stem Cells, 30 (2012) 2472–2486. [PubMed: 22887987]

[45]. Altaner C, Altanerova V, Cihova M, Ondicova K, Rychly B, Baciak L, Mravec B, Complete regression of glioblastoma by mesenchymal stem cells mediated prodrug gene therapy simulating clinical therapeutic scenario, Int J Cancer, 134 (2014) 1458–1465. [PubMed: 24038033]

[46]. Niess H, von Einem JC, Thomas MN, Michl M, Angele MK, Huss R, Gunther C, Nelson PJ, Bruns CJ, Heinemann V, Treatment of advanced gastrointestinal tumors with genetically modified autologous mesenchymal stromal cells (TREAT-ME1): study protocol of a phase I/II clinical trial, BMC Cancer, 15 (2015)237. [PubMed: 25879229]

[47]. Dembinski JL, Wilson SM, Spaeth EL, Studeny M, Zompetta C, Samudio I, Roby K, Andreeff M, Marini FC, Tumor stroma engraftment of gene-modified mesenchymal stem cells as anti-tumor therapy against ovarian cancer, Cytotherapy, 15 (2013) 20–32. [PubMed: 23260083]

[48]. Bazhanov N, Ylostalo JH, Bartosh TJ, Tiblow A, Mohammadipoor A, Foskett A, Prockop DJ, Intraperitoneally infused human mesenchymal stem cells form aggregates with mouse immune cells and attach to peritoneal organs, Stem cell research & therapy, 7 (2016) 27. [PubMed: 26864573]

[49]. Pistollato F, Abbadi S, Rampazzo E, Persano L, Della Puppa A, Frasson C, Sarto E, Scienza R, D'Avella D, Basso G, Intratumoral hypoxic gradient drives stem cells distribution and MGMT expression in glioblastoma, Stem Cells, 28 (2010) 851–862. [PubMed: 20309962]

[50]. Zhao D, Najbauer J, Garcia E, Metz MZ, Gutova M, Glackin CA, Kim SU, Aboody KS, Neural stem cell tropism to glioma: critical role of tumor hypoxia, Mol Cancer Res, 6 (2008) 1819–1829. [PubMed: 19074827]

[51]. Jansen WJ, Kolfschoten GM, Erkelens CA, Van Ark-Otte J, Pinedo HM, Boven E, Anti-tumor activity of CPT-11 in experimental human ovarian cancer and human soft-tissue sarcoma, Int J Cancer, 73 (1997) 891–896. [PubMed: 9399672]

Highlights

- Targeted therapy of drug-resistant ovarian cancer by mesenchymal stem cells
- The engineered mesenchymal stem cells localized at tumor stroma/ necrotic regions
- The engineered mesenchymal stem cells converted irinotecan to SN-38
- The treatment approach yielded complete response and provided survival benefits
- No toxicity to major organs was observed (histopathology/hematology)

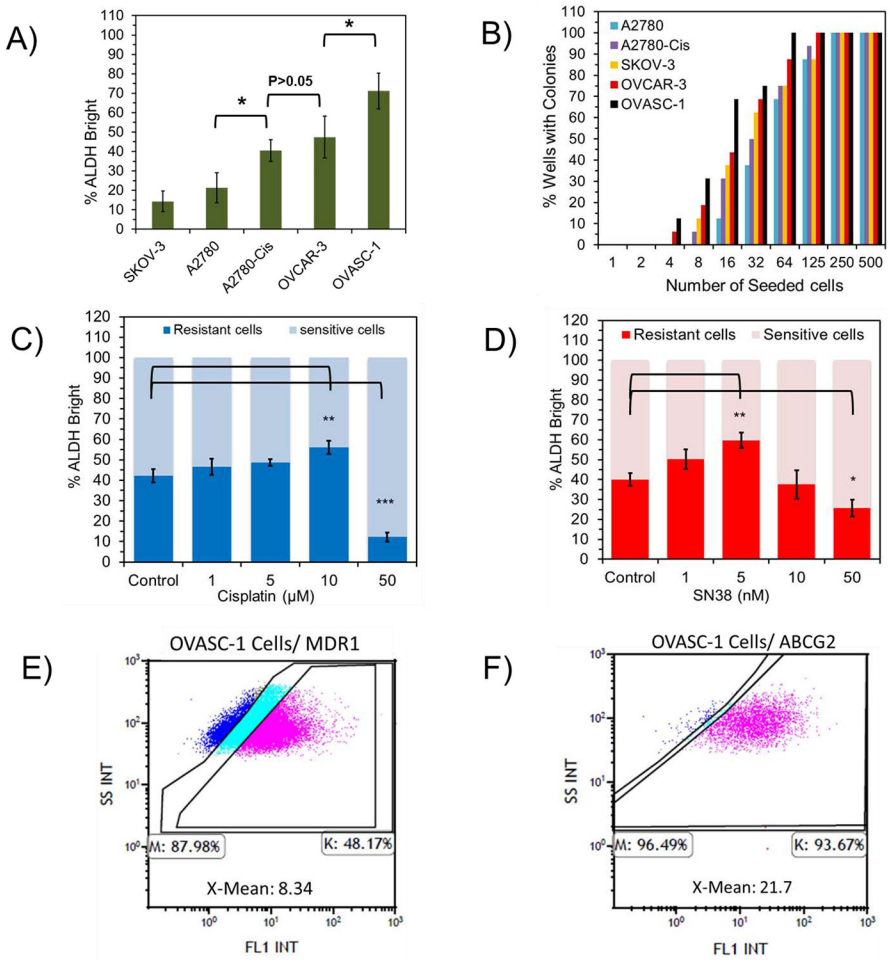

Figure 1:

Assessment of the percentages of drug-resistant cells and CICs. A) Determination of the percentage of the of ALDH+ (bright) cells in the general population of ovarian cancer cells by ALDH assay. B) Measurement of the percentage of the CICs in each ovarian cancer cell population by Limiting Dilution Assay. For details of data analysis, please see Figure S3B. C–D) Change in the percentage of ALDH+ cells in OVASC-1 cells after treatment with cisplatin (1–50 μM) and SN-38 (1–50 nM). The total number of cells (sensitive and resistant) as measured by flow cytometry is normalized to 100%. E-F) The percentages of OVASC-1 cells that express MDR1 and ABCG2 transporters. X-mean (Mean Fluorescence Intensity) denotes the fold difference in between the expression of the transporters on the surface of OVASC-1 cells stained by the anti-MDR1/anti-ABCG2 antibodies and by the IgG isotype control. This fold difference in X-Mean indicates the transporter density on the surface of the cells.

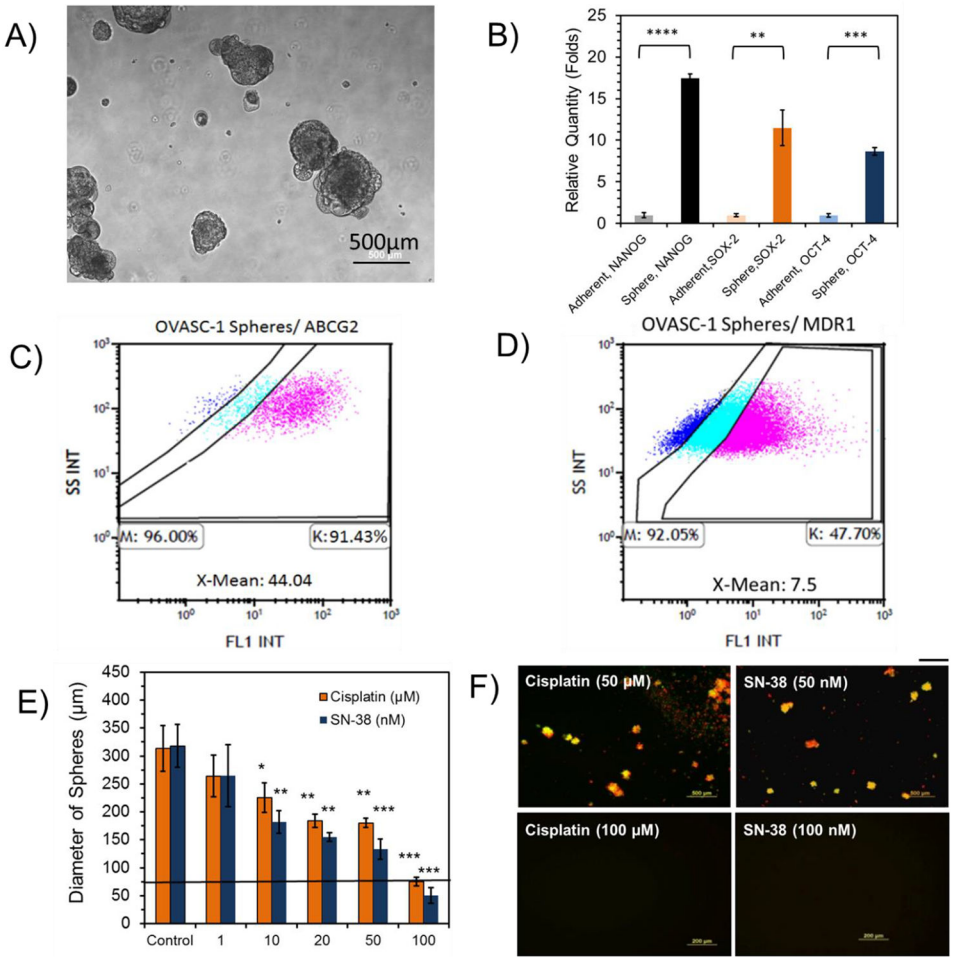

Figure 2:

Characterization and evaluation of the sensitivity of OVASC-1 tumorspheres to drugs. A) Formation of OVASC-1 tumorspheres in non-adherent plates. B) Measurement of typical stem cell biomarkers in OVASC-1 tumorspheres generated under non-adherent conditions and in comparison to cells cultured under adherent conditions. *Statistical significance, t-test (p<0.05). C-D) The percentages of cells that express ABCG2 and MDR1 transporters in OVASC-1 tumorspheres. X-mean denotes the fold difference in expression of the transporter on the surface of OVASC-1 cells stained by the anti-MDR1/anti-ABCG2 antibodies in comparison to the IgG isotype control indicating the transporter density. E) Measurement of the tumorspheres' diameters after treatment with SN-38 and cisplatin. Data are presented as mean±s.d. (n=4). F) Tumorspheres were stained with the fluorophores calcein-AM (CAM) and propidium iodide (PI) to visualize live (green) and dead (red) cells, respectively. Scale bar=500 µm.

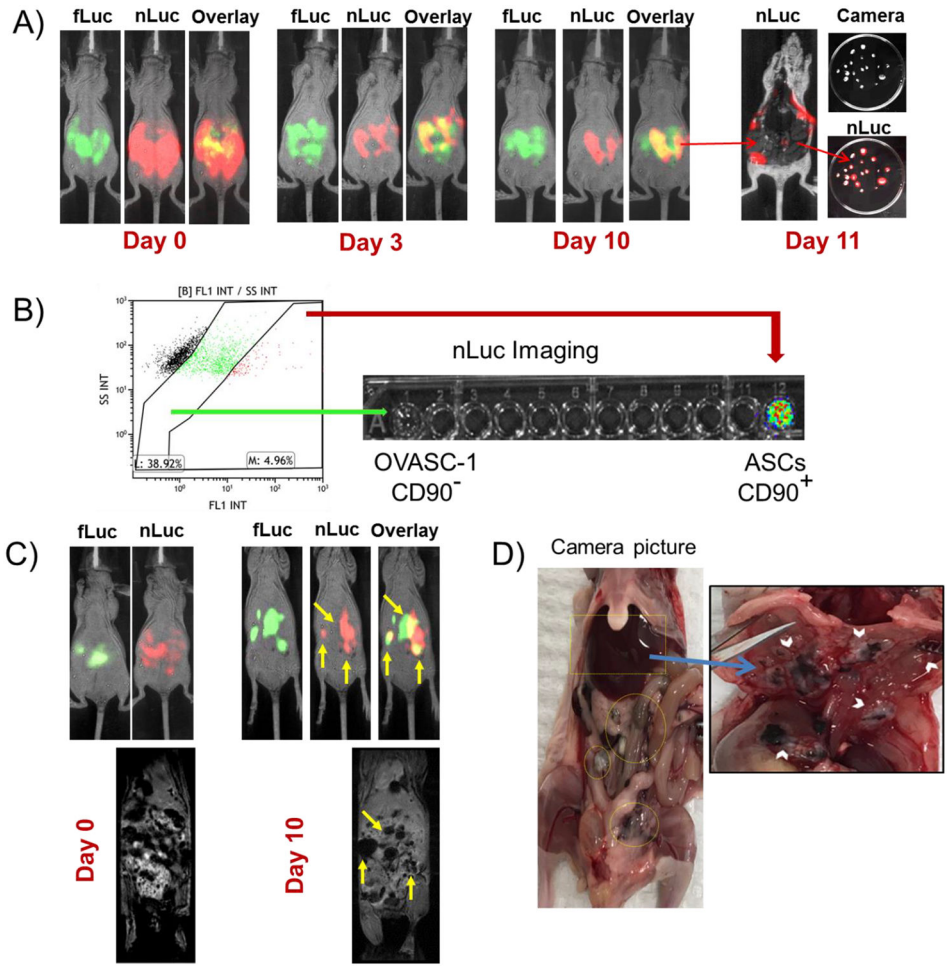

Figure 3:

Evaluation of the tumor tropism of ASC-shCE2:nLuc cells. A) BLI of nude mice with intraperitoneal OVASC-fLuc tumors (green) and ASC-shCE2:nLuc cells (red) over ten days. The co-localization of ASCs with OVASC-1 cells (yellow) could be observed as soon as three days. The excised tumors on day 11 showed expression of nLuc. B) Flow cytometry analysis of single cell suspension of extracted tumors labeled with anti-CD90 primary antibody. The CD90+ and CD90^{-} cells were then sorted into separate wells and incubated with furimazine and imaged for bioluminescence. C) BLI of the mouse with the intraperitoneal OVASC-1-fLuc tumors and the corresponding T2*-weighted MRI sequence of ASC-shCE2:nLuc-SP cells on days zero and ten. The tumors that were detectable by BLI could be marked by MRI with more accuracy. D) Camera picture of the dissected mouse abdomen with blackened tumor surfaces. The blackened tumors suggest presence of SPION nanoparticles.

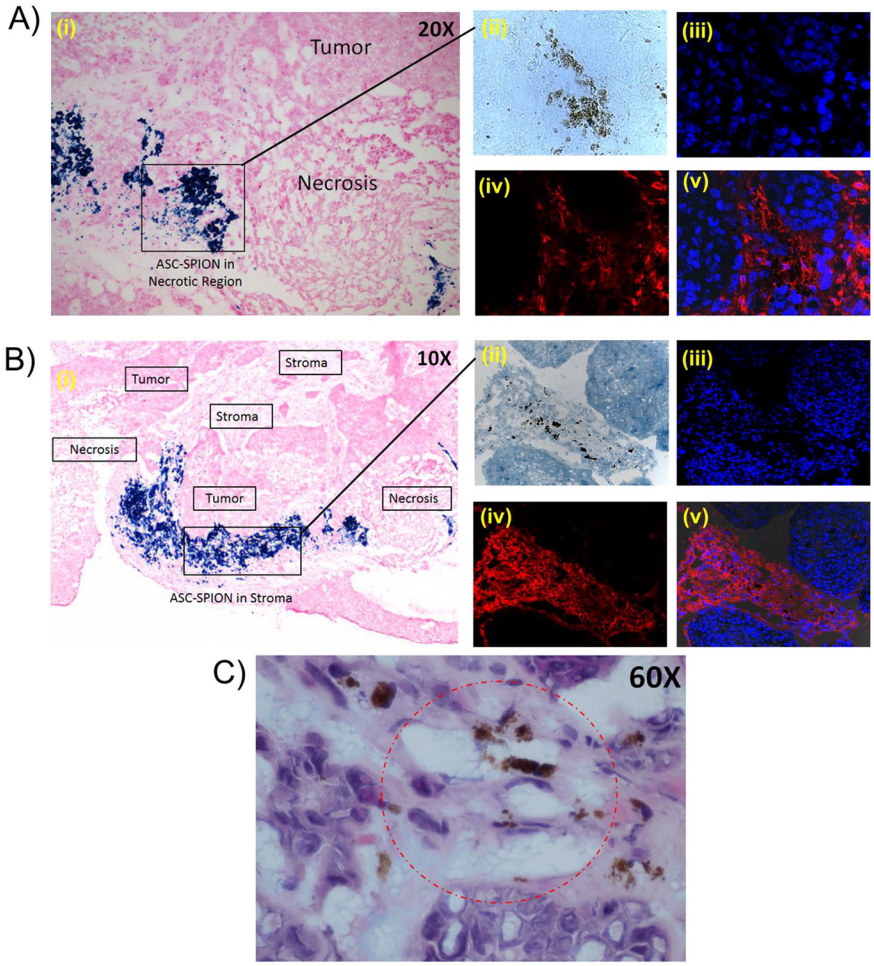

Figure 4:

Haemotoxylin and Eosin (H&E) staining, Prussian blue staining and CD90 labeling of sectioned tumor tissues. A-B) The tumor tissue sections under the microscope (10X and 20X magnification) showing localization of the ASC-shCE2:nLuc-SP cells in necrotic and stroma regions (i). The immunohistochemistry of the tumor tissue section and visualization under the fluorescent microscope (40X magnification); tumor tissue section under transmitted light showing presence of SPIONs in tumor tissues (ii), stained cell nucleus by DAPI showing the locations of cells in the field of view (iii), CD90+ cells stained by Texas Red in the same field of view (iv), and DAPI/Texas Red overlays showing the presence of numerous CD90+ cells among the $CD90^{-}$ cells (v). C) 60X magnification of tumor tissue section stained by H&E and Prussian Blue. The circled region shows the SPION-loaded ASCs with vacuolated cytoplasm within the tumor tissue.

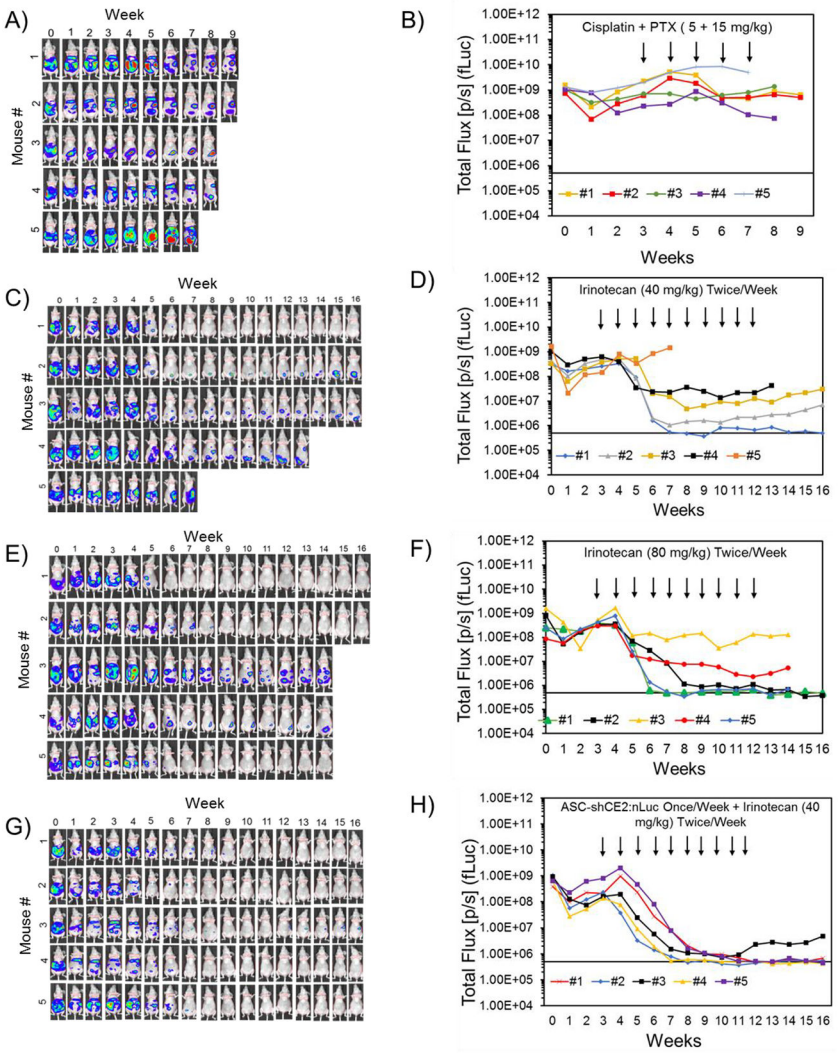

Figure 5:

Evaluation of therapy responses and cancer relapse by BLI (firefly luciferase imaging). BLI of nude mice with intraperitoneal tumors and quantitative analysis of signal in mice treated with: A-B) the standard-of-care regimen once a week (cisplatin+PTX); C-D) irinotecan (40 mg/kg) twice/week; E-F) irinotecan (80 mg/kg) twice/week; and G-H) ASC-shCE2:nLuc cells once a week and irinotecan (40 mg/kg) twice/week. The black arrows point at the weeks that mice received treatment. The baseline at 5×10^5 (p/s) shows the background bioluminescence of mice body without any tumors.

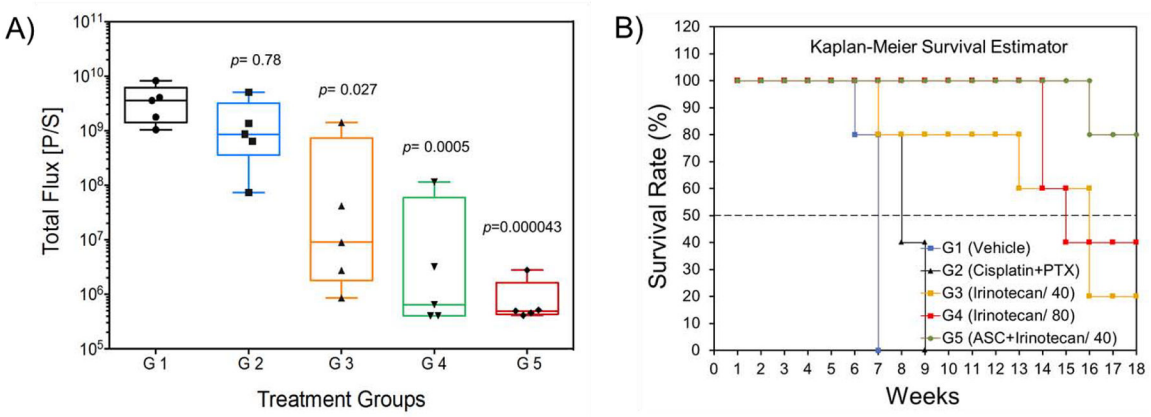

Figure 6:

A) Evaluation of the responses to therapy from the bioluminescence signal intensity (total flux) of the tumor burden observed immediately after the last treatment point. (*ANOVA, followed by Post hoc Tukey test). In this figure, the statistical significance (*p* value) is shown for G2 when compared to G1. G3, G4 and G5 are compared to G2 with the corresponding *p* values. B) Evaluation of survival benefit by Kaplan-Meier survival estimator. The survival rates for G1 to G5 were 0%, 0%, 20%, 40% and 80%, respectively. For details of the data analysis for this test please see Figure S22.

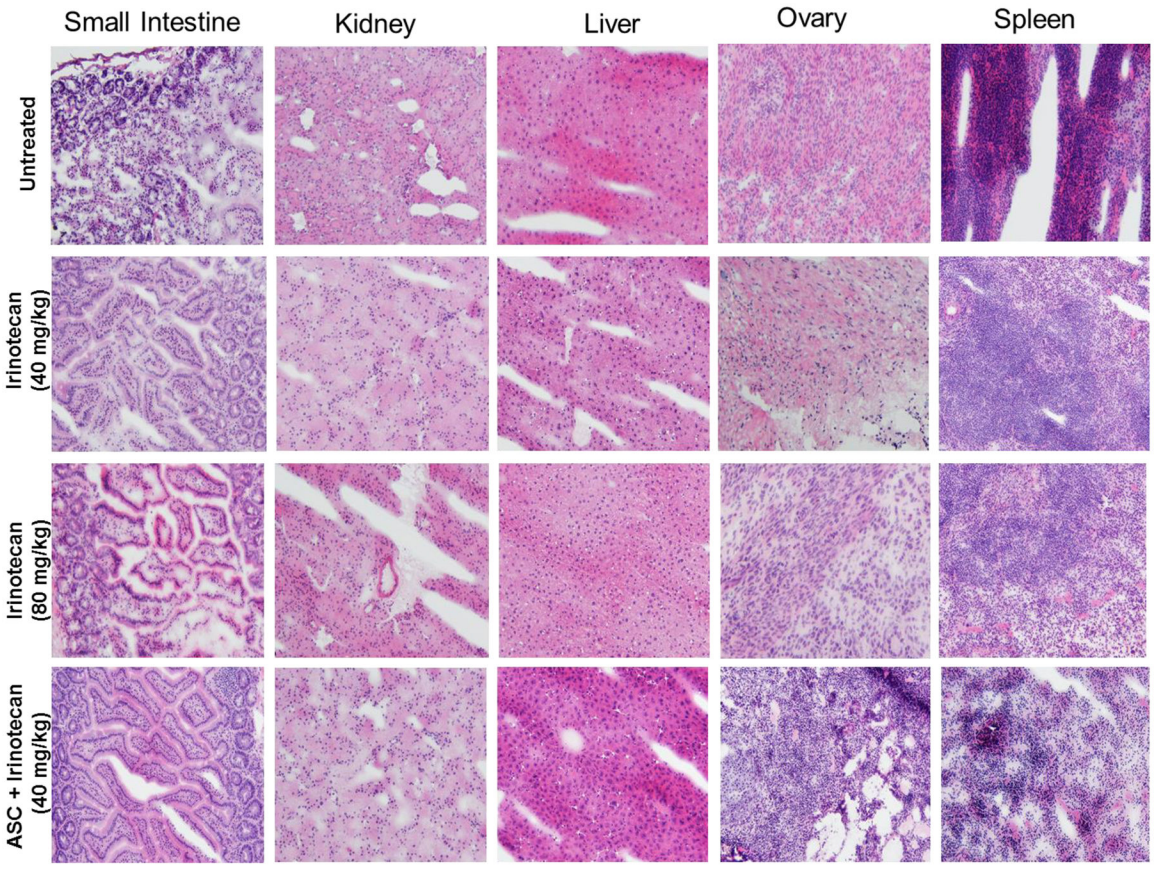

Figure 7:

Hematoxylin and eosin (H& E) staining of dissected mouse peritoneal organs. Photomicrography was conducted by using a Leica microscope with a 20X objective. Mice in different treatment groups showed no morphologic changes in major intraperitoneal organs reviewed as compared to control mice.

Table 1:

Determination of IC50 of anticancer drugs in different ovarian cancer cell lines based on the cell viability curves (Figure SI). The data show that OVASC-1 is the most drug-resistant cell line and SN-38 the most potent anticancer drug among the ones tested.

Drug/Cell Line	A2780	A2780-Cis	SKOV-3	OVCAR-3	OVASC-1
Cisplatin (μM)	1.1	15.69	9.1	11.78	19.75
6 Methylpurine (μM)	2.51	4.7	0.12	5.46	39.74
5 Fluorouracil (μM)	2.46	4.45	2.88	2.4	35.8
SN-38 (nM)	6.21	17.98	3.59	22.1	48.73

Table 2:

Stratification of mice into five treatment groups and evaluation of responses to therapy, toxicity, and recurrence. CR: complete response meaning no evidence of the tumor mass. PR: partial response meaning a decrease in tumor volume (≥25%). NR: no response meaning no significant decrease in tumor mass. Recurrence: increase in tumor mass after a complete or partial response. * Drug-related observable toxicity during treatment: More than 10% weight loss in a week or more than 20% weight loss over any time period; diarrhea, bulky ascites, distended abdomen, or lethargy.

Group	Treatment	Mice/group	CR	PR	NR	Treatment-Related Toxicity*	Recurrence
G1	Vehicle control	5	0	0	5	0	N/A
G2	Cisplatin+ Paclitaxel 5 + 15 (mg/kg)	5	0	0	5	0	N/A
G3	Irinotecan 40 (mg/kg)	5	1	3	1	0	3
G4	Irinotecan 80 (mg/kg)	5	3	2	0	3	2
G5	ASC-shCE2:nLuc + Irinotecan 40 (mg/kg)	5	4	1	0	0	1